iScience

Article

Pseudomonas aeruginosa aggregates elicit neutrophil swarming

Graphical abstract

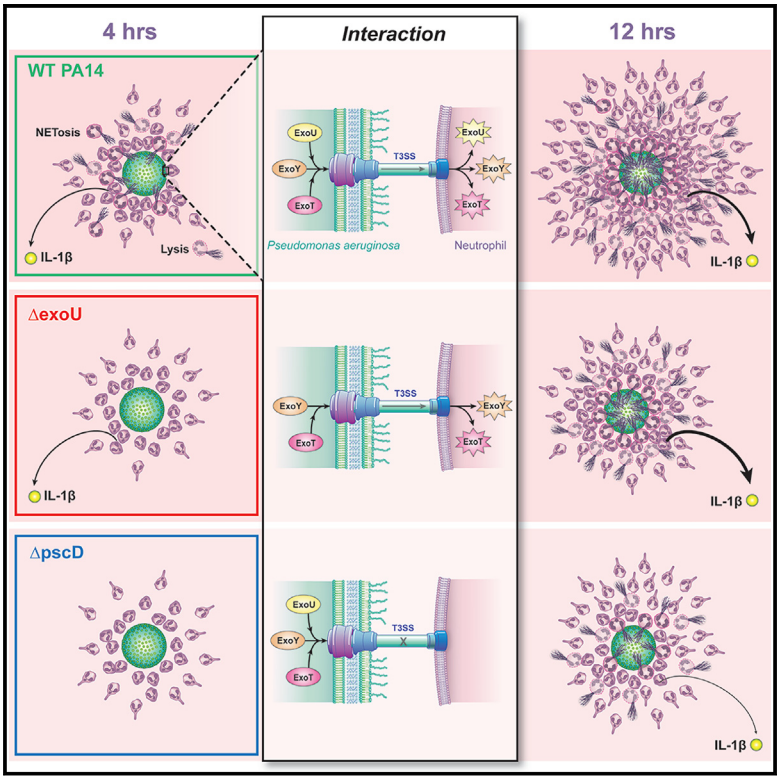

Highlights

- *Ex vivo* model elicits neutrophil swarming in response to bacterial aggregates
- Rapid and robust swarming response follows engagement with pathogenic targets
- *P. aeruginosa* T3SS components play critical role at eliciting neutrophil swarming
- NET activation and DNA release during swarm expansion are linked to T3SS secretion

Authors

Eliana Drenkard, Christian Godfrey, Alex Hopke, Sujatha Rajeev Thundivalappil, Michael Chen Li, Daniel Irimia, Bryan P. Hurley

Correspondence

dirimia@mgh.harvard.edu (D.I.), bphurley@mgh.harvard.edu (B.P.H.)

In brief

Microbiology; Medical Microbiology

Drenkard et al., 2025, iScience *28*, 111805
February 21, 2025
https://doi.org/10.1016/j.isci.2025.111805

CellPress

iScience

CellPress
OPEN ACCESS

Article

Pseudomonas aeruginosa aggregates elicit neutrophil swarming

Eliana Drenkard,[1,2,6] Christian Godfrey,[2,3,4,6] Alex Hopke,[2,3,4,5] Sujatha Rajeev Thundivalappil,[1,2] Michael Chen Li,[1,3,4] Daniel Irimia,[2,3,4,7,*] and Bryan P. Hurley[1,2,7,8,*]

[1]Mucosal Immunology and Biology Research Center, Massachusetts General Hospital, Boston MA 02114, USA
[2]Harvard Medical School, Boston, MA 02115, USA
[3]Center for Engineering in Medicine and Surgery, Massachusetts General Hospital, Boston, MA 02129, USA
[4]Shriners Hospital for Children, Boston, MA 02114, USA
[5]Present address: Alex Hopke, Department of Biomedical Sciences, East Tennessee State University Quillen College of Medicine, Center of Excellence in Inflammation, Infectious Disease and Immunity, East Tennessee State University, Johnson City, TN 37614, USA
[6]These authors contributed equally
[7]Senior author
[8]Lead contact
*Correspondence: dirimia@mgh.harvard.edu (D.I.), bphurley@mgh.harvard.edu (B.P.H.)
https://doi.org/10.1016/j.isci.2025.111805

SUMMARY

Pseudomonas aeruginosa, a gram-negative multidrug-resistant (MDR) opportunist, belongs to the ESKAPE group of pathogens associated with the highest risk of mortality. Neutrophil swarming is a host defense strategy triggered by larger threats, where neutrophil swarms contain and clear damage/infection. Current *ex vivo* models designed to study neutrophil-pathogen interactions largely focus on individual neutrophil engagement with bacteria and fail to capture neutrophil swarming. Here, we report an *ex vivo* model that reproducibly elicits neutrophil swarming in response to bacterial aggregates. A rapid and robust swarming response follows engagement with pathogenic targets. Components of the type III secretion system (T3SS), a critical *P. aeruginosa* virulence determinant, are involved in swarm interaction. This *ex vivo* approach for studying neutrophil swarming in response to large pathogen targets constitutes a valuable tool for elucidating host-pathogen interaction mechanisms and for evaluating novel therapeutics to combat MDR infections.

INTRODUCTION

Pseudomonas aeruginosa is a multidrug-resistant opportunistic pathogen that infects patients with epithelial injuries or impaired immune defenses and rarely affects healthy individuals. *P. aeruginosa* causes acute or chronic infections in immunocompromised patients with cystic fibrosis, chronic obstructive pulmonary disease, cancer, traumas, burns, sepsis, and ventilator-associated pneumonia.[1–3] This notorious opportunist is a frequent source of hospital-acquired infections and has been categorized as an ESKAPE pathogen.[4–6] ESKAPE pathogens are a group of prevalent species (*Enterococcus faecium*, *Staphylococcus aureus*, *Klebsiella pneumoniae*, *Acinetobacter baumannii*, *P. aeruginosa*, and *Enterobacter* spp.) that feature emerging strains characterized by resistance toward multiple classes of first-line and last-resort antibiotics. *P. aeruginosa* is ubiquitous in the environment and expresses a large and variable array of virulence factors that allow remarkable metabolic flexibility and adaptability to multiple conditions, including the host immune response. Virulence factor expression is tightly regulated to prevent deployment when not required.[7–9] One of the most important *P. aeruginosa* virulence factors is the type III secretion system (T3SS), a complex nanomachine found in many gram-negative bacteria. The T3SS forms a syringe-like structure, named injectisome, that is inserted into host cell membranes and injects effector proteins directly into the cytosol of infected cells.[10,11] Effector proteins then facilitate host colonization through the manipulation of host cell responses. Among the host pathways affected by T3SS are cell death (apoptosis, pyroptosis, and necroptosis), immune responses (nuclear factor κB [NF-κB], mitogen-activated protein kinase [MAPK], and inflammasome), as well as cytoskeletal and intracellular trafficking processes.[12,13]

Neutrophils are critical innate immune cells that mount fast and powerful responses against gram-negative pathogens like *P. aeruginosa*.[14] Studies of neutrophil engagement with *P. aeruginosa* have largely focused on the interactions between individual neutrophils and bacteria.[15,16] These investigations have revealed key neutrophil defense tactics, including the ability to engulf individual bacteria, exposing them to the phagolysosome and the capacity to release a variety of toxic mediators, including reactive oxygen species (ROS), reactive nitrogen species, antimicrobial peptides, and proteases.[16,17] Individual neutrophils were also shown to expel DNA, histones, and antimicrobial proteins, forming neutrophil extracellular traps (NETs) to thwart larger pathogenic threats.[17,18] In general, single

neutrophils acting independently can efficiently patrol and clear small microbes by engulfing and destroying them within phagolysosomes and by ensnaring them in individual-cell-released NETs.[17] When neutrophils encounter large microbial targets, like hyphae forming fungi or large areas of infected/damaged tissue, they employ a cooperative tactic called neutrophil swarming that synergizes neutrophil functions.[19]

Neutrophil swarming is an emergent behavior of communicating populations of neutrophils characterized a decade ago as a newly appreciated host innate immune mechanism that leverages the capability of neutrophils to work together in engaging large pathological threats.[20,21] Physical containment of the injured and/or infected tissues by large numbers of neutrophils is paired with a synergistically coordinated and focused deployment of the collective neutrophil arsenal to eradicate infection and remove damaged tissue.[20] As a defense strategy, neutrophil swarming attempts to achieve a delicate balance between threat elimination and preservation of surrounding healthy tissue.[20] During this population-driven response, neutrophils undergo sequential phases of highly directed chemotaxis, intercellular signal relay, and cluster formation.[22,23] Neutrophil secretion of chemokines and chemoattractants during the process leads to a self-amplifying swarming response that takes place in a feedforward manner, allowing intercellular communication and providing a level of self-organization to the swarm.[24] Effector functions of these dense clusters of hundreds of neutrophils collectively prevents pathogen escape, facilitates clearance, and promotes repair and healing processes.[25–29]

Much remains to be elucidated regarding the various mechanisms that regulate neutrophil swarming. Fungi are known triggers of neutrophil swarming, particularly as they transition toward a hyphal growth state[19,22] since fungal hyphae present a target too large for individual neutrophils to eliminate through phagocytosis. By comparison, significantly less is known about neutrophil swarming behavior against large bacterial targets such as biofilms. Swarming induced by bacteria-infected tissue in mice and zebrafish has been described *in vivo*[21,30] but experimental approaches to study neutrophil swarming of live bacterial targets *in vitro/ex vivo* are lacking. Bacteria form architecturally complex communities surrounded by an extracellular polymeric matrix of DNA, polysaccharides, lipids, and proteins,[31–33] which represent one of the most effective survival mechanisms of bacterial species in a variety of environments including within human hosts.[31,34] Studies of plaque biofilms in periodontal pockets revealed that individual neutrophils are ineffective at engulfing large biofilm structures *in vivo*. Instead, neutrophils form a "wall" between the junctional epithelium and the pathogen-rich dental plaque that can lead to progression of inflammatory periodontal disease due to the release of enzymes within neutrophil lysosomal granules, products of oxidative burst, and other pro-inflammatory substances directly into the pockets.[35] The cystic fibrosis airway is characterized by persistent infections with *P. aeruginosa* biofilms that lead to continuous bouts of neutrophilic infiltration and accumulation at the mucosa, where neutrophil swarming may represent a key feature of the chronic-infection-driven tissue inflammation observed in this disease process. Taken together, neutrophil swarming likely plays a crucial role in mucosal infections, particularly when tissue is colonized by pathogenic bacterial biofilms. Although it is reasonable to suggest that bacterial pathogens can serve as robust triggers for neutrophil swarming behavior, *in vitro/ex vivo* models and experimental systems to investigate this are lacking, and motile planktonic bacterial cultures are not compatible with existing *ex vivo* swarming platforms.

Here, we describe an *ex vivo* neutrophil swarming model that integrates *P. aeruginosa*-embedded agar beads as large bacterial biofilm-like stimuli with specialized micro-engineered platforms for the systematic analysis of neutrophil swarming behavior. We show that the model reproducibly delivers a rapid and robust neutrophil swarming response when encountering bacterial aggregates immobilized in agar beads. We also show that *P. aeruginosa* T3SS participates in the induction of neutrophil swarming. Overall, these results validate the use of this *ex vivo* approach for studying neutrophil swarming in response to large bacterial targets. The multiplexed design and controllability of the *ex vivo* model offer unprecedented opportunities to identify and characterize host and pathogen mediators that impact neutrophil swarming. Moreover, this model can be deployed to assess innovative therapeutics that bolster neutrophil swarming for the treatment of MDR infections when existing antibiotics are no longer effective.

RESULTS

P. aeruginosa-embedded beads induce a strong neutrophil swarming response

Upon initial preparation (T0) of live *P. aeruginosa*-embedded agar beads, fluorescent microscopy images showed that GFP-expressing bacteria were embedded throughout the entire bead (Figure 1A). After incubation of the beads in LB media for 20 h (T20), fluorescent microscopy images revealed that individual bacteria embedded in the agar had grown into aggregates or microcolonies that were now covering most of the bead surface (Figure 1A). The beads contained approximately 5×10^3 bacteria and measured between 100 and 200 μm. Images obtained using confocal microscopy showed dense bacterial growth on the surface and in the interior of the beads (Figure S1A and Video S1), thus representing large immobilized pathogenic targets potentially able to elicit a neutrophil swarming response. A series of microwell arrays were mounted on 12-well cell culture plates with glass bottoms to analyze the response of neutrophils to the *P. aeruginosa*-embedded beads. The microwell arrays were designed to keep bacterial beads in close contact with neutrophils and facilitate pathogen-neutrophil interactions. We assembled arrays of four 2-mm PDMS microwells on the glass surface of each well within the culture plates (Figure 1B). We then monitored the interaction between human neutrophils and wild-type *P. aeruginosa* strain PA14 (Table 1) beads using time-lapse microscopy over a 14-h period. We observed a rapid and robust swarming response within the first 30 min as reflected by dense regions of Hoechst-stained nuclei surrounding the live *P. aeruginosa* beads (Figure 1C; Videos S2 and S3). Quantitatively, the magnitude of neutrophil swarming induced by wild-type *P. aeruginosa* beads

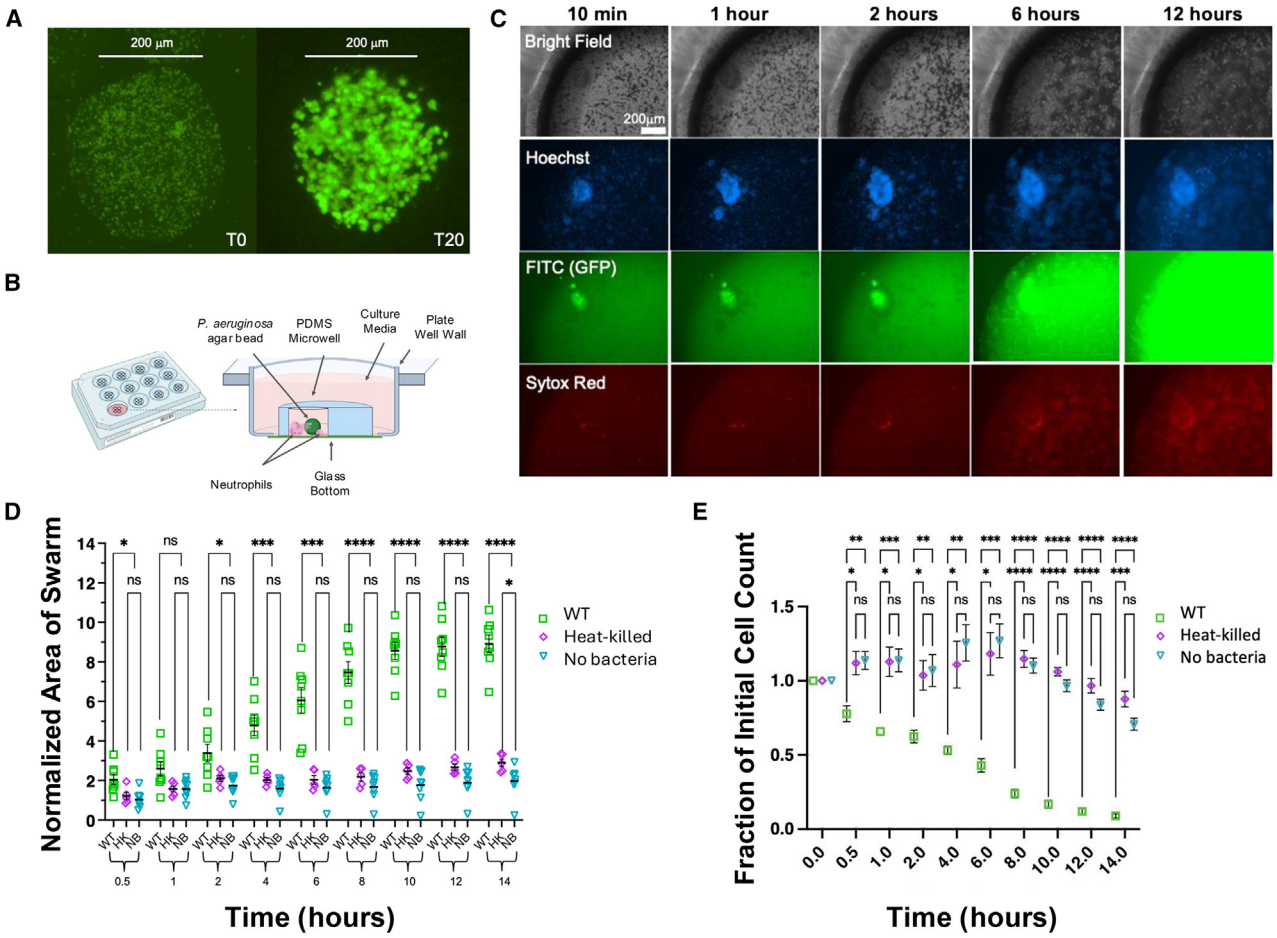

Figure 1. Neutrophil swarming response induced by *P. aeruginosa*-embedded agar beads

(A) Agar beads embedded with GFP-expressing *P. aeruginosa* were analyzed using fluorescent microscopy immediately after preparation (T0) and after incubation in sterile liquid LB media for 20-h (T20). Scale bar is 200 μm.

(B) Four PDMS microwell arrays were mounted into each well of a 12-well glass bottom plate to facilitate close contact between agar beads and neutrophils during image analysis..

(C) Images show progression of neutrophil swarming response induced by *P. aeruginosa* beads during 14-h time lapse. Images show Brightfield, Hoechst staining, GFP (green fluorescence), and Sytox Deep Red (red fluorescence). Scale bar is 200 μm.

(D) Areas of swarm were quantified over time after swarms were segmented manually using the image processing software FIJI. Dense regions of Hoechst-stained nuclei surrounding agar beads were used to identify swarm area boundaries. Beads embedded with heat-killed bacteria and no bacteria were examined for comparison. Intensity datapoints were normalized to the initial measurement.

(E) Cell quantification was performed using the cell segmentation algorithm Cellpose. The algorithm identified, segmented, and counted Hoechst-stained neutrophil nuclei within the images. Beads containing heat-killed bacteria, or no bacteria, were examined for comparison. Four independent replicates were performed for each experiment, and data are representative of three independent experiments. Error bars represent mean ± standard deviation. P values indicating significance are depicted as follows: *p < 0.05, **p < 0.01, ***p < 0.001, ****p < 0.0001, ns is non-significant.

increased over the first few hours but appeared to plateau over time (Figures 1C and 1D). In contrast, beads containing heat-killed bacteria or no bacteria failed to elicit a significant swarming response (Figure 1D). Areas of swarming elicited by wild-type PA14 beads were significantly larger than swarm areas formed in response to beads containing heat-killed bacteria or no bacteria over the 14-h period (Figure 1D), indicating that live pathogens are necessary to induce a neutrophil swarming response in this context. No significant differences were observed between the areas of the swarm elicited by heat-killed beads and beads without bacteria, aside from a slight increase at 14 h for heat-killed beads over beads alone (Figure 1D).

Beads embedded with *P. aeruginosa* strain PA14 impact *neutrophil* fate

Initial growth of the swarms elicited by live pathogen beads correlated with a steady increase in the number of incoming neutrophils as revealed by the surge in density of Hoechst-stained nuclei surrounding wild-type beads (Figures 1C and 1D; Videos S2 and S3). However, after the first few hours, swarm expansion appeared less associated with neutrophil recruitment and more

Table 1. Bacterial strains and plasmids used in this study

Strains/Plasmids	Relevant characteristic(s)	Reference or source
PA14-*gfp*	Virulent burn wound isolate of *P. aeruginosa* harboring pUCP19-*gfp*	Rahme et al.[59]
Δ*pscD*	Δ*pscD* (1.17-kb in-frame deletion of TTSS *pscD* gene)	Miyata et al.[38]
Δ*exoU*	Δ*exoU* (2.0-kb deletion of TTSS *exoU* gene)	Miyata et al.[38]
Δ*pscD-gfp*	Δ*pscD* harboring pUCP19-*gfp*	This study
Δ*exoU-gfp*	Δ*exoU* harboring pUCP19-*gfp*	This study
Plasmids		
pUCP19-*gfp*	Polylinker *lacZ*, lac^{iq} selection, *bla, gfp*	Zhang et al.[65]

a consequence of increased dissipation of Hoechst-stained nuclei (Figure 1D; Videos S2 and S3). Diffuse nuclear material across the field of view was evident after 5–6 h of incubation (Figure 1C; Videos S2 and S3), suggesting that neutrophils were undergoing cell death. In parallel, we observed rapid growth of GFP-expressing *P. aeruginosa* beginning at 6 h of incubation (Figure 1C). We used Sytox Deep Red Nucleic Acid Stain to detect the presence of extracellular nuclear material as an indicator of cellular disruption and an indirect way to monitor NETosis, a process that leads to the formation of NETs. NETosis is a host defense mechanism where neutrophils deliberately expel DNA decorated with antimicrobial proteins to capture and kill extracellular pathogens.[18] We determined that as swarm expansion progresses in response to wild-type beads, a marked increase in the release of extracellular DNA is observed, consistent with enhanced NETosis (Figure 1C). We next used the cell segmentation algorithm Cellpose to analyze nuclei integrity and quantify neutrophils from captured Hoechst-stained images (Figure 1C). A representative frame from Hoechst-stained time-lapse imaging shows neutrophils adjacent to wild-type beads rapidly disappearing and/or losing nuclear integrity to a much larger extent than neutrophils adjacent to beads containing heat-killed bacteria or beads without bacteria (Figure S1B). Quantitatively, Cellpose analysis shows a steady decline in cell counts for neutrophils proximal to live wild-type beads over the 14-h incubation period as reflected by complete loss of nuclei or nuclei integrity among most of the neutrophils analyzed (Figure 1E). Neutrophil counts indicate that neutrophils were actively dying or moving out of frame toward the swarm foci during incubation with beads that contained live *P. aeruginosa* (Figures 1C and S1B). In contrast, neutrophils incubated with beads containing either heat-killed bacteria or no bacteria showed minimal viability loss or out-of-frame movement during the 14-h incubation (Figures 1E and S1B). Counts of neutrophils incubated in the absence of beads did not change significantly throughout the 14-h incubation (Figure S1C).

P. aeruginosa type III secretion system is critical to elicit neutrophil swarming and neutrophil cell death

There is a direct link between T3SS-dependent pathogen invasion, survival, persistence, and damage caused to host tissues. The T3SS and its effectors are involved in a variety of mechanisms that result in host cell damage, including direct cytotoxicity by inducing apoptosis or necrosis, and indirect damage by causing tissue barrier disruptions.[11,36,37] To investigate the role of T3SS in neutrophil swarming and associated neutrophil cell death, we analyzed the effect of inactivating two *P. aeruginosa* T3SS genes. The *pscD* gene encodes an essential component of the

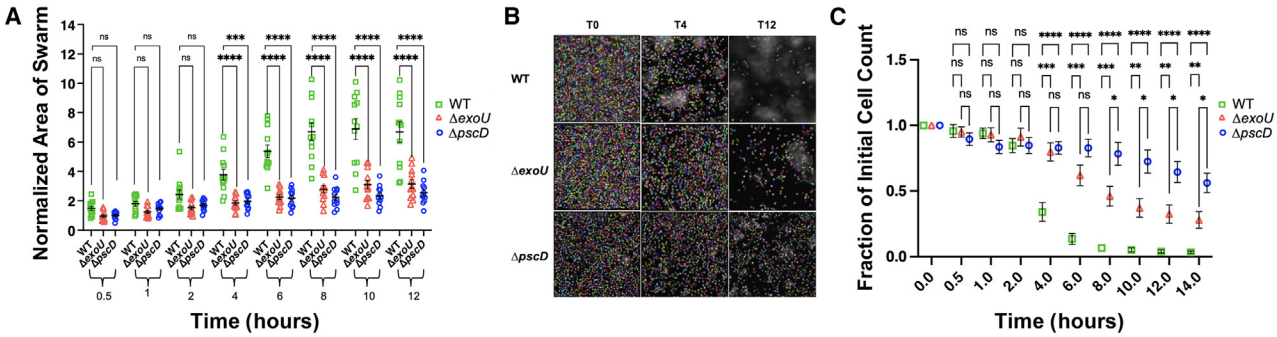

Figure 2. Role of *P. aeruginosa* T3SS in neutrophil swarming response and neutrophil cell death

(A) Areas of swarm were imaged over 14 h in assays performed with beads containing wild-type, Δ*exoU* and Δ*pscD* mutants. Intensity datapoints were normalized to the initial measurement.

(B) Images obtained using Hoechst-stained time-lapse imaging show neutrophils incubated with wild-type, Δ*exoU* and Δ*pscD* mutant beads. Cellpose frames show segmented neutrophil nuclei identified with pixel-level labels for quantification of neutrophil cell loss.

(C) Cell death quantification was performed using the cell segmentation algorithm Cellpose during swarming interaction with *P. aeruginosa* beads. Beads containing wild-type, Δ*exoU* and Δ*pscD* mutants were used in swarming assays. Four independent replicates were done for each experiment, and data are representative of three independent experiments. Error bars represent mean ± standard deviation. P values indicating significance are depicted as follows: *p < 0.05, **p < 0.01, ***p < 0.001, ****p < 0.0001, ns is non-significant.

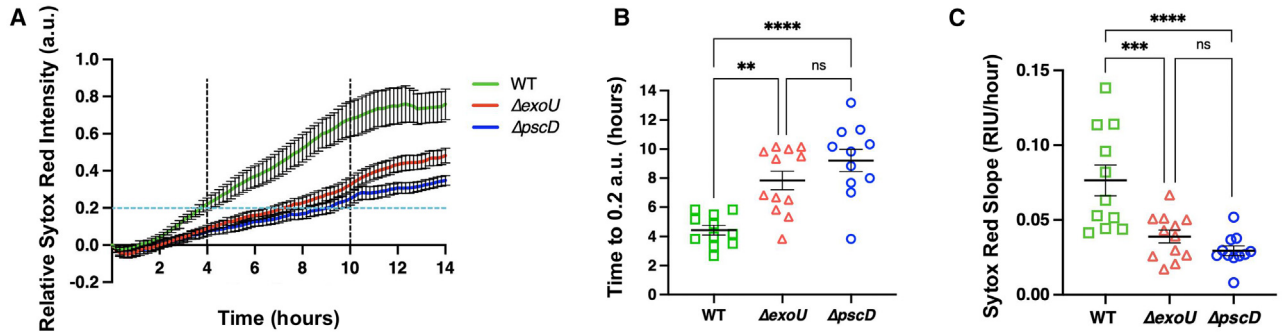

Figure 3. Role of *P. aeruginosa* T3SS in neutrophil cell death

(A) Sytox Deep Red stain was used to quantify extracellular nuclear material as an indicator of neutrophil cell death. Intensity profiles were measured within each time-lapse frame and plotted over time. Intensity datapoints were normalized to the initial measurement. Biological replicates of each condition were averaged for graphical representation. Vertical dotted lines indicate the time frame for rapid swarm expansion (4–10 h).

(B) Comparison of time point at which relative Sytox Deep Red intensity reaches 0.2 a.u. (arbitrary units) during swarm assays using wild-type, Δ*exoU* and Δ*pscD* beads.

(C) Sytox Red Slope analysis during rapid swarm expansion showing rate of DNA release. Four independent replicates were performed for each experiment, and data are representative of three independent experiments. Error bars represent mean ± standard deviation. P values indicating significance are depicted as follows: **p < 0.01, ***p < 0.001, ****p < 0.0001, ns is non-significant.

injectisome basal body, and its inactivation prevents secretion of all effector proteins along with other T3SS extracellular components.[38] The second gene is *exoU*, which encodes the most potently cytotoxic effector protein delivered into host cells by the T3SS. Analysis of neutrophil engagement with T3SS mutant beads Δ*exoU* and Δ*pscD* (Table 1) revealed swarm areas considerably smaller than elicited by wild-type beads, where significant differences were distinguishable by 4 h (Figure 2A). Importantly, beads containing mutant bacteria did not appear to display any observable differences when compared to wild-type beads, as assessed by fluorescent microscopy (Figure S2A). When comparing swarm areas elicited by the mutant beads (Δ*exoU* vs. Δ*pscD*), we found significantly larger swarms formed after 8 h of neutrophil engagement with Δ*exoU* (Figure S2B). Cellpose cell count analysis revealed that Δ*exoU* and Δ*pscD* mutant beads triggered loss of neutrophils and/or nuclei integrity significantly later than wild-type beads. Nuclei integrity and/or neutrophil loss was evident after just 4 h of incubation with wild-type beads, which was not observed in neutrophils incubated with T3SS mutant beads at the same time point (Figures 2B and 2C). Neutrophil counts proximal to Δ*exoU* beads decreased to a larger extent than counts proximal to Δ*pscD* beads by 6 h, as Δ*exoU* beads appeared to cause a greater loss of cells than Δ*pscD* beads. This difference continued to persist throughout the period of analysis, with Δ*pscD* beads eliciting only modest neutrophil loss throughout the 14-h analysis (Figures 2B and 2C). Quantification of extracellular nuclear material using Sytox Deep Red stain suggests that neutrophils incubated with wild-type beads released DNA more rapidly compared to neutrophils incubated with mutant beads, reaching an arbitrarily established threshold of 0.2 a.u. at approximately

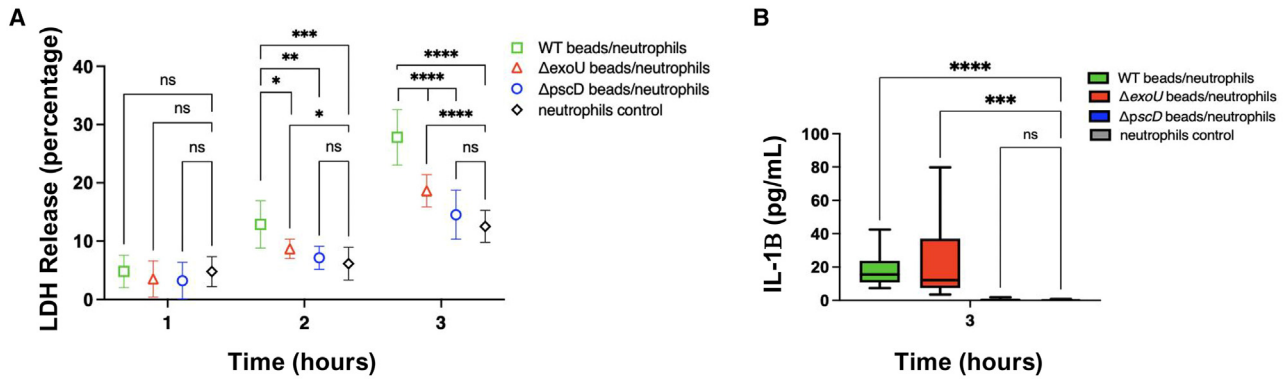

Figure 4. Role of T3SS in cell lysis and production of IL-1β during neutrophil swarming response

(A) LDH release was used to assess neutrophil cell lysis. Cytotoxicity was expressed as percentage of total amount of LDH released in culture supernatants.

(B) Quantification of cytokine IL-1β was done using an enzyme-linked immunosorbent assay. Measurements of LDH release and production of IL-1β were done using supernatants from swarming assays performed using wild-type, Δ*exoU* and Δ*pscD* beads. Four independent replicates were done for each experiment, and data are representative of three independent experiments. Error bars represent mean ± standard deviation. P values indicating significance are depicted as follows: *p < 0.05, **p < 0.01, ***p < 0.001, ****p < 0.0001, ns is non-significant.

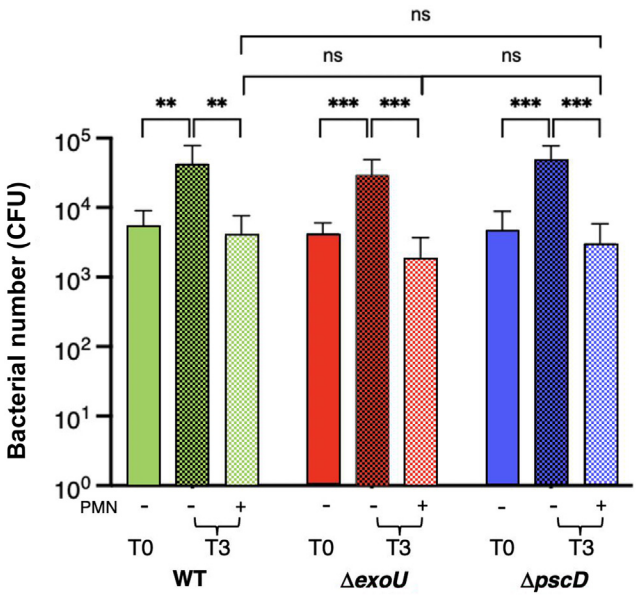

Figure 5. Survival of *P. aeruginosa* bacteria during interaction with neutrophil swarms

Bacterial survival was quantified by counting CFUs after 3-h incubation of bacteria-embedded beads and neutrophils (PMN). Samples containing *P. aeruginosa* beads without neutrophils were used as negative controls. Data correspond to the average ±SD of four independent replicates per condition representative of three independent experiments ($N = 12$). Comparisons between groups were performed using two-tailed Student's t test. $p < 0.05$ was considered significant. P values indicating significance are depicted as follows: **p < 0.01, ***p < 0.001, ns is non-significant.

4 h post-incubation (Figures 3A and 3B). Slope analysis of Sytox Red intensity during rapid swarm expansion (4–10 h) indicates significantly enhanced velocity and overall magnitude of DNA release for wild-type beads compared to mutant beads (Figure 3C). Although no significant differences were observed between mutant beads during Sytox Red analysis (Figure 3), slope analysis done at the later stages of the swarming observation period (10–14 h) showed that Δ*exoU* beads clearly elicited enhance magnitude and velocity of extracellular DNA release compared with Δ*pscD* beads at later stages of the interaction (Figures S2C and S2D).

Release of lactate dehydrogenase (LDH) following damage of the plasma membrane is a feature of cell death processes and represents a distinct approach to quantify neutrophil viability during engagement with *P. aeruginosa* beads. Wild-type beads triggered significantly more neutrophil LDH release as early as 2 h compared with neutrophils incubated in the absence of beads (Figure 4A). Mutant *ΔexoU* beads also elicited neutrophil cell death, but LDH release values were significantly lower than wild-type beads at 2 and 3 h (Figure 4A). Mutant Δ*pscD* beads did not elicit a significant increase in LDH release above background over the 3-h incubation period (Figure 4A). When assessing LDH release following extended periods of incubation (9 h), neutrophils exposed to wild-type beads exhibited nearly 80% of maximal LDH release (Figure S3A). Beads from both mutants did elicit LDH release from neutrophils at 9 h when compared to neutrophils incubated without beads, but the percentage of LDH release was significantly diminished compared to levels observed from neutrophils exposed to wild-type beads.

IL-1β release is triggered by neutrophil engagement with *P. aeruginosa* beads

Interleukin-1β (IL-1β) is a potent pro-inflammatory cytokine that is crucial for host-defense responses to infection and injury.[39] Quantitation of IL-1β revealed a significant increase in cytokine production in samples containing wild-type and mutant *ΔexoU* beads compared to neutrophils alone, whereas mutant Δ*pscD* beads failed to trigger IL-1β production by neutrophils after 3 h incubation (Figure 4B). However, a significant, albeit moderate production of IL-1β was observed in neutrophils exposed to Δ*pscD* mutant beads after 9 h of incubation (Figure S3B).

Neutrophil swarms *restrict* bacterial growth at early stages of interaction with *P. aeruginosa* beads

We quantified the impact that neutrophil swarms have on the viability of bacteria embedded in agar beads after 3 h of co-incubation by disrupting the agar beads and counting colony-forming units (CFUs). Results show that neutrophil swarms effectively limit the growth of bacteria during the early stages of these interactions (3 h), and this effect is independent of the strain used to prepare the beads (Figure 5). After 3 h of incubation, bacterial numbers increased approximately 1 log in the no-neutrophil controls, but this increase in CFUs was not observed when neutrophils were co-incubated with the beads (Figure 5). As demonstrated earlier, neutrophils are observed to be actively swarming at this time point (Figure 2A). Despite notable differences in the magnitude of neutrophil swarming elicited by wild-type and T3SS mutant beads, no significant differences in the capacity of neutrophil swarms to impede bacterial growth are evident (Figure 5). Importantly, CFUs recovered from wild-type and T3SS mutant beads do not show significant differences at T0, indicating that wild-type and mutant beads are qualitatively (Figure S2A) and quantitatively (Figure 5) similar.

DISCUSSION

We developed and validated an *ex vivo* model that facilitates the analysis of neutrophil swarming induced by large target structures of the pathogen *P. aeruginosa*. Current models designed to study neutrophil swarm interactions *in vitro* utilize microarray printing platforms that contain large clusters of live pathogens.[22,40] Although this approach is effective at generating targets for non-motile or heat-killed organisms (e.g., *Candida albicans* spores and *S. aureus*, respectively),[22,41] it is not compatible for assessment of live motile bacterial species. To overcome this obstacle, we adapted an approach previously developed to immobilize bacteria in agar beads[42] and then induced formation of sessile biofilm-like aggregates throughout the beads, thus creating a large pathogenic target capable of inducing a robust neutrophil swarming response. The present approach expands the application of microscale technologies to the study of neutrophil swarm interactions with large sessile aggregates of motile pathogen species offering a unique opportunity to analyze cellular and molecular mechanisms as well as

the kinetics of neutrophil swarm formation. Importantly, this model could become a valuable tool to develop studies of interactions between neutrophil swarms and biofilms.

Biofilms are complex multicellular communities highly resistant to both immune responses and antibiotic treatment that account for 80% of chronic and recurrent microbial infections in humans. Reports show that *P. aeruginosa* biofilms are protected from individual neutrophil infiltration during ocular infections in mice.[43,44] Neutrophils reach the border of biofilm structures but are unable to easily penetrate them, hindering the ability of neutrophils to phagocytose biofilm bacteria.[43–45] Kugadas et al. (2019) reported the presence of neutrophil swarms approaching bacterial biofilms, suggesting that neutrophil swarming is induced as a response to biofilm infections. However, a detailed characterization of the interaction between neutrophil swarms and biofilms has not been reported to date. Analysis of mechanisms involved in neutrophil swarm/biofilm interactions has significant potential to broaden the scope of therapeutic strategies designed to combat MDR infections and associated inflammatory pathologies by highlighting novel paths to develop immune-based therapies.

Components of *P. aeruginosa* T3SS play a critical role at eliciting neutrophil swarming, as beads containing T3SS mutants Δ*exoU* and Δ*pscD* elicit a much weaker swarming response than wild-type beads. The ExoU toxin, a ubiquitin-activated phospholipase A_2 (PLA_2) associated with rapid cellular lysis, and PscD, an essential protein of the injectisome basal body, both play a dominant role in induction of neutrophil swarming, despite causing rapid host cell cytotoxicity. Injectisome impairment in mutant Δ*pscD*, which results in inability to secrete T3SS effector proteins including ExoU,[38] has a much stronger effect on swarming than *exoU* gene inactivation, suggesting further involvement of additional effector proteins beyond ExoU and/or the injectisome itself in swarming induction that precedes neutrophil cell death. Two additional effectors proteins known to be secreted by the T3SS of *P. aeruginosa* strain PA14 are ExoT and ExoY. ExoT has been shown to inhibit NLRC4 inflammasome activation, leading to decrease inflammatory response,[46] and ExoY is an actin-activated nucleotidyl cyclase that impacts the actin cytoskeleton.[47,48] ExoY has been reported to attenuate proinflammatory cytokine production by downregulating the activation of transforming-growth-factor-activated kinase 1 (TAK1), NF-κB, and MAPK kinases.[49] The role of the ExoT and ExoY effector proteins in neutrophil swarming remains to be determined.

The T3SS injectisome itself seems to play an important role at triggering release of the inflammasome mediator IL-1β, which is supported by our observation that Δ*pscD* mutant beads failed to trigger release of the IL-1β cytokine at early stages of engagement with neutrophils. This result is consistent with reports showing that human neuronal apoptosis inhibitory protein (NAIP) isoforms sense the T3SS inner rod and needle from multiple bacterial species,[50] leading to inflammasome activation. *P. aeruginosa* T3SS inner-rod protein PscI and needle protein PscF are both sensed by the hNAIP-NLRC4 inflammasome, resulting in caspase-1 and IL-1β maturation and a robust inflammatory response.[51]

Alternatively, differences in neutrophil induction observed between the Δ*exoU* and Δ*pscD* mutant beads could also be explained by a hypothesis that postulates the existence of T3SS effector codependency and context-dependent effector essentiality. Simultaneous deletion of multiple effectors in *Citrobacter rodentium* revealed that T3SS effectors operate as an interconnected network *in vivo*, emphasizing the importance of performing studies of the role of individual T3SS effectors in the context of the entire effector network.[52] T3SS effectors in *Salmonella Typhimurium* have also been shown to function as a network, contributing to the ability of the pathogen to colonize and spread into different host tissues.[53]

Induction of neutrophil cell death associated with cell loss, extracellular DNA release, and LDH release is also dependent on *P. aeruginosa* T3SS. This is consistent with the reported role of *P. aeruginosa* T3SS in induction of necrosis and apoptosis in macrophages,[54] cytotoxicity in neutrophils,[55] and destruction of intracellular membranes leading to rapid cell necrosis associated with ExoU translocation.[56,57] Inflammatory responses, evidenced by increased production of IL-1β, and homeostatic death processes triggered by uncontrolled release of toxic substances from dead neutrophils could also contribute to further neutrophil death.[58] Thus, neutrophil cell death induced during the swarm response could result from a combination of mechanisms related to bacterial pathogenesis and host immune responses.

NET activation and extracellular DNA release as swarm expansion progresses is associated with translocation of toxins and secretion of T3SS effectors, which agrees with the role played by the release of T3SS toxins in triggering NET formation during interaction between *P. aeruginosa* biofilms and human neutrophils in ocular infections.[44] Formation of a NETs barrier or "dead-zone" around infecting biofilms was associated with release of ExoS, a toxin secreted by *P. aeruginosa* strain PAO1, which is not present in strain PA14. Although this NETs barrier contributed to restrict *P. aeruginosa* dissemination into the brain, it also promoted antibiotic resistance in bacteria and led to severe local ulcerative damage to the eye. Interestingly, mice infected with the *exoS* mutant show no apparent formation of a "dead-zone," and neutrophils were able to penetrate biofilms.[44] The role of the ExoS effector in swarming interactions between neutrophils and *P. aeruginosa* beads will be the focus of future research.

The results presented in this study reveal a key role for T3SS in driving the neutrophil swarming response. The process is also accompanied by accelerated neutrophil cell death associated with production of T3SS toxins and potentially mechanisms triggered by the innate immune response. Systematic characterization of host pathways that initiate, orchestrate, and resolve the swarming process as well as bacterial mechanisms involved in the interaction with neutrophil swarms will be critical to develop effective therapeutic alternatives targeting MDR infections.

Limitations of the study

Although the *ex vivo* model described in this manuscript reveals a considerable amount of novel interplay and crosstalk between neutrophils with their swarming response when engaged with pathogenic *P. aeruginosa* aggregates, the model lacks the host tissue component that would be present *in vivo* where bacteria

colonize to launch the infection and summon neutrophils. To reconcile and validate certain findings from our model to an actual *in vivo* infection may require additional model refinements that also incorporate the infected host mucosal tissue.

RESOURCE AVAILABILITY

Lead contact

Requests for further information and resources should be directed to and will be fulfilled by the lead contact, Bryan Hurley (bphurley@mgh.harvard.edu).

Materials availability

This study did not generate any new unique reagents. Slides and plates for the swarming assays are available through the BioMEMS Core at the Massachusetts General Hospital https://researchcores.partners.org/biomem/about.

Data and code availability

- All data reported in this article are publicly available as of the date of publication. Accession numbers are listed in the key resources table or from the lead contact on request.
- This article does not report any original code.
- Any additional information required to reanalyze the data reported in this article is listed in the KRT or from the lead contact on request.

ACKNOWLEDGMENTS

The authors thank Liakot Khan and Yihan Zhang for technical assistance with confocal microscope and Bobby J. Cherayil for critical review of the manuscript. Graphical Abstract is illustrated by Nicole Wolf, MS, ©2024 (nicolecwolf@gmail.com). The authors acknowledge funding from the National Institutes of Health (NIH/NIAID AI176658 to D.I. and AI095338 to B.P.H.), Shriners Hospitals for Children (71010-BOS-22 to D.I.), and the MGH ECOR ISF (B.P.H.). Support for M.C.L. was provided by the MGfC Digestive Disease Summer Research Program (NIH/NIDDK DK103579 to B.P.H.).

AUTHOR CONTRIBUTIONS

Conceptualization, E.D., A.H., D.I., and B.P.H.; investigation, E.D., C.G., A.H., S.R.T., and M.C.L.; writing—original draft, E.D.; writing—review and editing, E.D., C.G., A.H., S.R.T., D.I., and B.P.H.; supervision, D.I. and B.P.H.; funding acquisition, D.I. and B.P.H.

DECLARATION OF INTERESTS

Author BPH and DI are Guest Editors for the Swarming across the biological spectrum Special Issue published in iScience.

STAR★METHODS

Detailed methods are provided in the online version of this paper and include the following:

SUPPLEMENTAL INFORMATION

Supplemental information can be found online at https://doi.org/10.1016/j.isci.2025.111805.

Received: July 29, 2024
Revised: September 3, 2024
Accepted: January 10, 2025
Published: January 11, 2025

REFERENCES

1. Cendra, M.D.M., and Torrents, E. (2021). Pseudomonas aeruginosa biofilms and their partners in crime. Biotechnol. Adv. *49*, 107734. https://doi.org/10.1016/j.biotechadv.2021.107734.
2. Jurado-Martin, I., Sainz-Mejias, M., and McClean, S. (2021). Pseudomonas aeruginosa: An Audacious Pathogen with an Adaptable Arsenal of Virulence Factors. Int. J. Mol. Sci. *22*, 3128. https://doi.org/10.3390/ijms22063128.
3. Rossi, E., La Rosa, R., Bartell, J.A., Marvig, R.L., Haagensen, J.A.J., Sommer, L.M., Molin, S., and Johansen, H.K. (2021). Pseudomonas aeruginosa adaptation and evolution in patients with cystic fibrosis. Nat. Rev. Microbiol. *19*, 331–342. https://doi.org/10.1038/s41579-020-00477-5.
4. Boucher, H.W., Talbot, G.H., Bradley, J.S., Edwards, J.E., Gilbert, D., Rice, L.B., Scheld, M., Spellberg, B., and Bartlett, J. (2009). Bad bugs, no drugs: no ESKAPE! An update from the Infectious Diseases Society of America. Clin. Infect. Dis. *48*, 1–12. https://doi.org/10.1086/595011.
5. Gipson, K.S., Nickerson, K.P., Drenkard, E., Llanos-Chea, A., Dogiparthi, S.K., Lanter, B.B., Hibbler, R.M., Yonker, L.M., Hurley, B.P., and Faherty, C.S. (2020). The Great ESKAPE: Exploring the Crossroads of Bile and Antibiotic Resistance in Bacterial Pathogens. Infect. Immun. *88*, e00865-19. https://doi.org/10.1128/IAI.00865-19.
6. Nathwani, D., Raman, G., Sulham, K., Gavaghan, M., and Menon, V. (2014). Clinical and economic consequences of hospital-acquired resistant and multidrug-resistant Pseudomonas aeruginosa infections: a systematic review and meta-analysis. Antimicrob. Resist. Infect. Control *3*, 32. https://doi.org/10.1186/2047-2994-3-32.
7. Behzadi, P., Barath, Z., and Gajdacs, M. (2021). It's Not Easy Being Green: A Narrative Review on the Microbiology, Virulence and Therapeutic Prospects of Multidrug-Resistant Pseudomonas aeruginosa. Antibiotics *10*, 42. https://doi.org/10.3390/antibiotics10010042.
8. Qin, S., Xiao, W., Zhou, C., Pu, Q., Deng, X., Lan, L., Liang, H., Song, X., and Wu, M. (2022). Pseudomonas aeruginosa: pathogenesis, virulence factors, antibiotic resistance, interaction with host, technology advances and emerging therapeutics. Signal Transduct. Targeted Ther. *7*, 199. https://doi.org/10.1038/s41392-022-01056-1.
9. Sanchez-Jimenez, A., Llamas, M.A., and Marcos-Torres, F.J. (2023). Transcriptional Regulators Controlling Virulence in Pseudomonas aeruginosa. Int. J. Mol. Sci. *24*, 11895. https://doi.org/10.3390/ijms241511895.
10. Foulkes, D.M., McLean, K., Haneef, A.S., Fernig, D.G., Winstanley, C., Berry, N., and Kaye, S.B. (2019). Pseudomonas aeruginosa Toxin ExoU as a Therapeutic Target in the Treatment of Bacterial Infections. Microorganisms *7*, 707. https://doi.org/10.3390/microorganisms7120707.
11. Horna, G., and Ruiz, J. (2021). Type 3 secretion system of Pseudomonas aeruginosa. Microbiol. Res. *246*, 126719. https://doi.org/10.1016/j.micres.2021.126719.
12. Hardy, K.S., Tessmer, M.H., Frank, D.W., and Audia, J.P. (2021). Perspectives on the Pseudomonas aeruginosa Type III Secretion System Effector ExoU and Its Subversion of the Host Innate Immune Response to Infection. Toxins *13*, 880. https://doi.org/10.3390/toxins13120880.

13. Jouault, A., Saliba, A.M., and Touqui, L. (2022). Modulation of the immune response by the Pseudomonas aeruginosa type-III secretion system. Front. Cell. Infect. Microbiol. *12*, 1064010. https://doi.org/10.3389/fcimb.2022.1064010.

14. Koh, A.Y., Priebe, G.P., Ray, C., Van Rooijen, N., and Pier, G.B. (2009). Inescapable need for neutrophils as mediators of cellular innate immunity to acute Pseudomonas aeruginosa pneumonia. Infect. Immun. *77*, 5300–5310. https://doi.org/10.1128/IAI.00501-09.

15. Rada, B. (2017). Interactions between Neutrophils and Pseudomonas aeruginosa in Cystic Fibrosis. Pathogens *6*, 10. https://doi.org/10.3390/pathogens6010010.

16. Yonker, L.M., Cigana, C., Hurley, B.P., and Bragonzi, A. (2015). Host-pathogen interplay in the respiratory environment of cystic fibrosis. J. Cyst. Fibros. *14*, 431–439. https://doi.org/10.1016/j.jcf.2015.02.008.

17. Amulic, B., Cazalet, C., Hayes, G.L., Metzler, K.D., and Zychlinsky, A. (2012). Neutrophil function: from mechanisms to disease. Annu. Rev. Immunol. *30*, 459–489. https://doi.org/10.1146/annurev-immunol-020711-074942.

18. Xuan, N., Zhao, J., Kang, Z., Cui, W., and Tian, B.P. (2023). Neutrophil extracellular traps and their implications in airway inflammatory diseases. Front. Med. *10*, 1331000. https://doi.org/10.3389/fmed.2023.1331000.

19. Hopke, A., Lin, T., Scherer, A.K., Shay, A.E., Timmer, K.D., Wilson-Mifsud, B., Mansour, M.K., Serhan, C.N., Irimia, D., and Hurley, B.P. (2022). Transcellular biosynthesis of leukotriene B(4) orchestrates neutrophil swarming to fungi. iScience *25*, 105226. https://doi.org/10.1016/j.isci.2022.105226.

20. Glaser, K.M., Mihlan, M., and Lämmermann, T. (2021). Positive feedback amplification in swarming immune cell populations. Curr. Opin. Cell Biol. *72*, 156–162. https://doi.org/10.1016/j.ceb.2021.07.009.

21. Lammermann, T., Afonso, P.V., Angermann, B.R., Wang, J.M., Kastenmuller, W., Parent, C.A., and Germain, R.N. (2013). Neutrophil swarms require LTB4 and integrins at sites of cell death *in vivo*. Nature *498*, 371–375. https://doi.org/10.1038/nature12175.

22. Hopke, A., Scherer, A., Kreuzburg, S., Abers, M.S., Zerbe, C.S., Dinauer, M.C., Mansour, M.K., and Irimia, D. (2020). Neutrophil swarming delays the growth of clusters of pathogenic fungi. Nat. Commun. *11*, 2031. https://doi.org/10.1038/s41467-020-15834-4.

23. Reategui, E., Jalali, F., Khankhel, A.H., Wong, E., Cho, H., Lee, J., Serhan, C.N., Dalli, J., Elliott, H., and Irimia, D. (2017). Microscale arrays for the profiling of start and stop signals coordinating human-neutrophil swarming. Nat. Biomed. Eng. *1*, 0094. https://doi.org/10.1038/s41551-017-0094.

24. Kienle, K., and Lämmermann, T. (2016). Neutrophil swarming: an essential process of the neutrophil tissue response. Immunol. Rev. *273*, 76–93. https://doi.org/10.1111/imr.12458.

25. Irimia, D. (2020). Neutrophil Swarms Are More Than the Accumulation of Cells. Microbiol. Insights *13*, 1178636120978272. https://doi.org/10.1177/1178636120978272.

26. Lammermann, T. (2016). In the eye of the neutrophil swarm-navigation signals that bring neutrophils together in inflamed and infected tissues. J. Leukoc. Biol. *100*, 55–63. https://doi.org/10.1189/jlb.1MR0915-403.

27. Mihlan, M., Glaser, K.M., Epple, M.W., and Lämmermann, T. (2022). Neutrophils: Amoeboid Migration and Swarming Dynamics in Tissues. Front. Cell Dev. Biol. *10*, 871789. https://doi.org/10.3389/fcell.2022.871789.

28. Rocha-Gregg, B.L., and Huttenlocher, A. (2021). Swarming motility in host defense. Science *372*, 1262–1263. https://doi.org/10.1126/science.abj3065.

29. Song, Z., Bhattacharya, S., Clemens, R.A., and Dinauer, M.C. (2023). Molecular regulation of neutrophil swarming in health and disease: Lessons from the phagocyte oxidase. iScience *26*, 108034. https://doi.org/10.1016/j.isci.2023.108034.

30. Poplimont, H., Georgantzoglou, A., Boulch, M., Walker, H.A., Coombs, C., Papaleonidopoulou, F., and Sarris, M. (2020). Neutrophil Swarming in Damaged Tissue Is Orchestrated by Connexins and Cooperative Calcium Alarm Signals. Curr. Biol. *30*, 2761–2776. https://doi.org/10.1016/j.cub.2020.05.030.

31. Lopez, D., Vlamakis, H., and Kolter, R. (2010). Biofilms. Cold Spring Harbor Perspect. Biol. *2*, a000398. https://doi.org/10.1101/cshperspect.a000398.

32. Ma, L.Z., Wang, D., Liu, Y., Zhang, Z., and Wozniak, D.J. (2022). Regulation of Biofilm Exopolysaccharide Biosynthesis and Degradation in Pseudomonas aeruginosa. Annu. Rev. Microbiol. *76*, 413–433. https://doi.org/10.1146/annurev-micro-041320-111355.

33. Thi, M.T.T., Wibowo, D., and Rehm, B.H.A. (2020). Pseudomonas aeruginosa Biofilms. Int. J. Mol. Sci. *21*, 8671. https://doi.org/10.3390/ijms21228671.

34. Sharma, S., Mohler, J., Mahajan, S.D., Schwartz, S.A., Bruggemann, L., and Aalinkeel, R. (2023). Microbial Biofilm: A Review on Formation, Infection, Antibiotic Resistance, Control Measures, and Innovative Treatment. Microorganisms *11*, 1614. https://doi.org/10.3390/microorganisms11061614.

35. Scott, D.A., and Krauss, J. (2012). Neutrophils in periodontal inflammation. Front. Oral Biol. *15*, 56–83. https://doi.org/10.1159/000329672.

36. Finck-Barbancon, V., Goranson, J., Zhu, L., Sawa, T., Wiener-Kronish, J.P., Fleiszig, S.M., Wu, C., Mende-Mueller, L., and Frank, D.W. (1997). ExoU expression by Pseudomonas aeruginosa correlates with acute cytotoxicity and epithelial injury. Mol. Microbiol. *25*, 547–557. https://doi.org/10.1046/j.1365-2958.1997.4891851.x.

37. Hauser, A.R. (2009). The type III secretion system of Pseudomonas aeruginosa: infection by injection. Nat. Rev. Microbiol. *7*, 654–665. https://doi.org/10.1038/nrmicro2199.

38. Miyata, S., Casey, M., Frank, D.W., Ausubel, F.M., and Drenkard, E. (2003). Use of the Galleria mellonella caterpillar as a model host to study the role of the type III secretion system in Pseudomonas aeruginosa pathogenesis. Infect. Immun. *71*, 2404–2413. https://doi.org/10.1128/IAI.71.5.2404-2413.2003.

39. Chen, K.W., Groß, C.J., Sotomayor, F.V., Stacey, K.J., Tschopp, J., Sweet, M.J., and Schroder, K. (2014). The neutrophil NLRC4 inflammasome selectively promotes IL-1beta maturation without pyroptosis during acute Salmonella challenge. Cell Rep. *8*, 570–582. https://doi.org/10.1016/j.celrep.2014.06.028.

40. Hopke, A., and Irimia, D. (2020). Ex Vivo Human Neutrophil Swarming Against Live Microbial Targets. Methods Mol. Biol. *2087*, 107–116. https://doi.org/10.1007/978-1-0716-0154-9_8.

41. Kienle, K., Glaser, K.M., Eickhoff, S., Mihlan, M., Knöpper, K., Reátegui, E., Epple, M.W., Gunzer, M., Baumeister, R., Tarrant, T.K., et al. (2021). Neutrophils self-limit swarming to contain bacterial growth *in vivo*. Science *372*, eabe7729. https://doi.org/10.1126/science.abe7729.

42. Facchini, M., De Fino, I., Riva, C., and Bragonzi, A. (2014). Long term chronic Pseudomonas aeruginosa airway infection in mice. J. Vis. Exp. *85*, 51019. https://doi.org/10.3791/51019.

43. Kugadas, A., Geddes-McAlister, J., Guy, E., DiGiandomenico, A., Sykes, D.B., Mansour, M.K., Mirchev, R., and Gadjeva, M. (2019). Frontline Science: Employing enzymatic treatment options for management of ocular biofilm-based infections. J. Leukoc. Biol. *105*, 1099–1110. https://doi.org/10.1002/JLB.4HI0918-364RR.

44. Thanabalasuriar, A., Scott, B.N.V., Peiseler, M., Willson, M.E., Zeng, Z., Warrener, P., Keller, A.E., Surewaard, B.G.J., Dozier, E.A., Korhonen, J.T., et al. (2019). Neutrophil Extracellular Traps Confine Pseudomonas aeruginosa Ocular Biofilms and Restrict Brain Invasion. Cell Host Microbe *25*, 526–536. https://doi.org/10.1016/j.chom.2019.02.007.

45. Geddes-McAlister, J., Kugadas, A., and Gadjeva, M. (2019). Tasked with a Challenging Objective: Why Do Neutrophils Fail to Battle Pseudomonas aeruginosa Biofilms. Pathogens *8*, 283. https://doi.org/10.3390/pathogens8040283.

46. Mohamed, M.F., Gupta, K., Goldufsky, J.W., Roy, R., Callaghan, L.T., Wetzel, D.M., Kuzel, T.M., Reiser, J., and Shafikhani, S.H. (2022). CrkII/Abl phosphorylation cascade is critical for NLRC4 inflammasome activity

and is blocked by Pseudomonas aeruginosa ExoT. Nat. Commun. *13*, 1295. https://doi.org/10.1038/s41467-022-28967-5.

47. Beckert, U., Wolter, S., Hartwig, C., Bähre, H., Kaever, V., Ladant, D., Frank, D.W., and Seifert, R. (2014). ExoY from Pseudomonas aeruginosa is a nucleotidyl cyclase with preference for cGMP and cUMP formation. Biochem. Biophys. Res. Commun. *450*, 870–874. https://doi.org/10.1016/j.bbrc.2014.06.088.
48. Belyy, A., Mechold, U., Renault, L., and Ladant, D. (2018). ExoY, an actin-activated nucleotidyl cyclase toxin from P. aeruginosa: A minireview. Toxicon *149*, 65–71. https://doi.org/10.1016/j.toxicon.2017.12.046.
49. He, C., Zhou, Y., Liu, F., Liu, H., Tan, H., Jin, S., Wu, W., and Ge, B. (2017). Bacterial Nucleotidyl Cyclase Inhibits the Host Innate Immune Response by Suppressing TAK1 Activation. Infect. Immun. *85*, e00239-17. https://doi.org/10.1128/IAI.00239-17.
50. Reyes Ruiz, V.M., Ramirez, J., Naseer, N., Palacio, N.M., Siddarthan, I.J., Yan, B.M., Boyer, M.A., Pensinger, D.A., Sauer, J.D., and Shin, S. (2017). Broad detection of bacterial type III secretion system and flagellin proteins by the human NAIP/NLRC4 inflammasome. Proc. Natl. Acad. Sci. USA *114*, 13242–13247. https://doi.org/10.1073/pnas.1710433114.
51. Grandjean, T., Boucher, A., Thepaut, M., Monlezun, L., Guery, B., Faudry, E., Kipnis, E., and Dessein, R. (2017). The human NAIP-NLRC4-inflammasome senses the Pseudomonas aeruginosa T3SS inner-rod protein. Int. Immunol. *29*, 377–384. https://doi.org/10.1093/intimm/dxx047.
52. Sanchez-Garrido, J., Ruano-Gallego, D., Choudhary, J.S., and Frankel, G. (2022). The type III secretion system effector network hypothesis. Trends Microbiol. *30*, 524–533. https://doi.org/10.1016/j.tim.2021.10.007.
53. Chen, D., Burford, W.B., Pham, G., Zhang, L., Alto, L.T., Ertelt, J.M., Winter, M.G., Winter, S.E., Way, S.S., and Alto, N.M. (2021). Systematic reconstruction of an effector-gene network reveals determinants of Salmonella cellular and tissue tropism. Cell Host Microbe *29*, 1531–1544.e9. https://doi.org/10.1016/j.chom.2021.08.012.
54. Hauser, A.R., and Engel, J.N. (1999). Pseudomonas aeruginosa induces type-III-secretion-mediated apoptosis of macrophages and epithelial cells. Infect. Immun. *67*, 5530–5537. https://doi.org/10.1128/IAI.67.10.5530-5537.1999.
55. Rosen, H. (2004). Bacterial responses to neutrophil phagocytosis. Curr. Opin. Hematol. *11*, 1–6. https://doi.org/10.1097/00062752-200401000-00002.
56. Phillips, R.M., Six, D.A., Dennis, E.A., and Ghosh, P. (2003). In vivo phospholipase activity of the Pseudomonas aeruginosa cytotoxin ExoU and protection of mammalian cells with phospholipase A2 inhibitors. J. Biol. Chem. *278*, 41326–41332. https://doi.org/10.1074/jbc.M302472200.
57. Sato, H., Frank, D.W., Hillard, C.J., Feix, J.B., Pankhaniya, R.R., Moriyama, K., Finck-Barbançon, V., Buchaklian, A., Lei, M., Long, R.M., et al. (2003). The mechanism of action of the Pseudomonas aeruginosa-encoded type III cytotoxin, ExoU. EMBO J. *22*, 2959–2969. https://doi.org/10.1093/emboj/cdg290.
58. Bertheloot, D., Latz, E., and Franklin, B.S. (2021). Necroptosis, pyroptosis and apoptosis: an intricate game of cell death. Cell. Mol. Immunol. *18*, 1106–1121. https://doi.org/10.1038/s41423-020-00630-3.
59. Rahme, L.G., Stevens, E.J., Wolfort, S.F., Shao, J., Tompkins, R.G., and Ausubel, F.M. (1995). Common virulence factors for bacterial pathogenicity in plants and animals. Science *268*, 1899–1902. https://doi.org/10.1126/science.7604262.
60. Schneider, C.A., Rasband, W.S., and Eliceiri, K.W. (2012). NIH Image to ImageJ: 25 years of image analysis. Nat. Methods *9*, 671–675. https://doi.org/10.1038/nmeth.2089.
61. Schindelin, J., Arganda-Carreras, I., Frise, E., Kaynig, V., Longair, M., Pietzsch, T., Preibisch, S., Rueden, C., Saalfeld, S., Schmid, B., et al. (2012). Fiji: an open-source platform for biological-image analysis. Nat. Methods *9*, 676–682. https://doi.org/10.1038/nmeth.2019.
62. Pachitariu, M., and Stringer, C. (2022). Cellpose 2.0: how to train your own model. Nat. Methods *19*, 1634–1641. https://doi.org/10.1038/s41592-022-01663-4.
63. Stringer, C., Wang, T., Michaelos, M., and Pachitariu, M. (2021). Cellpose: a generalist algorithm for cellular segmentation. Nat. Methods *18*, 100–106. https://doi.org/10.1038/s41592-020-01018-x.
64. F.M. Ausubel, R. Brent, R.E. Kingston, D.D. Moore, J.G. Seidman, J.A. Smith, and K. Struhl, eds. (1992). Short protocols in molecular biology.
65. Zhang, S., Chen, Y., Potvin, E., Sanschagrin, F., Levesque, R.C., McCormack, F.X., and Lau, G.W. (2005). Comparative signature-tagged mutagenesis identifies Pseudomonas factors conferring resistance to the pulmonary collectin SP-A. PLoS Pathog. *1*, 259–268. https://doi.org/10.1371/journal.ppat.0010031.

STAR★METHODS

KEY RESOURCES TABLE

REAGENT or RESOURCE	SOURCE	IDENTIFIER
Bacterial and virus strains		
P. aeruginosa PA14-*gfp*	*Pseudomonas aeruginosa* isolate from patient (Rahme et al.[59]) harboring pUCP19-*gfp*	*P. aeruginosa,* strain UCBPP-PA14-*gfp*
P. aeruginosa PA14 Δ*exoU*	Miyata et al. 2003[38]	*P. aeruginosa* PA14 Δ*exoU*3
P. aeruginosa PA14 Δ*pscD*	Miyata et al. 2003[38]	*P. aeruginosa* PA14 Δ*pscD*8
P. aeruginosa PA14 Δ*exoU-gfp*	This article	Pa_PA14_Δ*exoU_gfp*
P. aeruginosa PA14 Δ*pscD-gfp*	This article	Pa_PA14_Δ*pscD_gfp*
Chemicals, peptides, and recombinant proteins		
Carbenicillin Disodium Salt	Teknova	C2113
Heavy mineral oil	Sigma-Aldrich	330760
Phosphate-buffered saline (PBS)	Gibco Thermo Fisher	10010049
Hoechst stain	Thermo Fisher Scientific	62249
Iscove Modified Dulbecco's Medium (IMDM)	Gibco (Thermo Fisher)	21056-023
Fetal Bovine Serum (FBS)	Gibco (Thermo Fisher)	10082147
SYTOX Deep Red Nucleic Acid Stain	Invitrogen	S11381
Triton X-100	Sigma-Aldrich	T8787
Critical commercial assays		
EasySep Direct Human Neutrophil isolation kit	Stemcell Technologies	19666
LDH Cytotoxicity Assay Kit	Thermo Fisher Scientific	C20301
DuoSet Human IL-1 β/IL-IF2	R&D Systems	DY201-05
Deposited data		
Data reported	This article	LabArchives https://doi.org/10.25833/p0cr-fd70
Software and algorithms		
3D Viewer plugin in FIJI	Schneider et al. 2012[60]	https://imagej.net/plugins/3d-viewer/
FIJI (distribution of ImageJ2 core)	Schindelin et al. 2012[61]	https://imagej.net/software/fiji/
Cellpose (v2.2.2)	Pachitariu et al. 2022, Stringer et al. 2021[62,63]	https://www.cellpose.org/
Other		
Conical polypropylene sterile 15mL centrifuge tubes	Thermo Fisher Scientific	339653
Sterile tissue culture 6-well plates	Thermo Fisher Scientific	FB12927
Glass bottom 12-well plates N° 1.5 coverslip uncoated	MatTek Corporation	P12G-1.5-14-F
Polydimethylsiloxane (PDMS) sheets of 3 mm thickness	Dow Corning	DOWC25100445
ProPlate Multi-Array 16-well slide system	Grace Bio-Labs	204860
Flat bottom 96-well plates	Thermo Fisher Scientific	12-565-501
Flat bottom sterile 96-well plates	Thermo Fisher Scientific	269787
Screw-cap 2mL microcentrifuge tubes	VWR International	16466-060

EXPERIMENTAL MODEL DETAILS

Bacterial strains

P. aeruginosa, strain UCBPP-PA14[59] expressing green fluorescence protein (*gfp*), and mutants *P. aeruginosa* PA14 Δ*exoU* and *P. aeruginosa* PA14 Δ*pscD*[38] were kindly provided by Fred M. Ausubel at the Department of Molecular Biology, Massachusetts General Hospital/Harvard Medical School. Bacterial strains were grown at 37°C in Luria-Bertani (LB) broth[64] supplemented with 300 μg/mL carbenicillin (Research Products International).

METHOD DETAILS

Bacterial strains

The bacterial strains and plasmids used in this study are listed in Table 1. Bacterial strains were routinely cultured in Luria-Bertani (LB) broth[64] supplemented with 300 μg/mL carbenicillin (Research Products International). Green fluorescent protein (GFP)-expressing *P. aeruginosa* strains were used in all swarming experiments. Plasmid pUCP19GFP (GFP^+ Ap^r), which constitutively expresses GFP, was introduced into *P. aeruginosa* strains by electroporation as previously described.[64]

Preparation of *P. aeruginosa* embedded agar beads

The protocol used to prepare *P. aeruginosa*-embedded agar beads was adapted from a method designed to study chronic *P. aeruginosa* airway infections in mice.[42] Overnight cultures of GFP-expressing *P. aeruginosa* strains were diluted 1:100 in LB media containing 300 μg/mL carbenicillin and incubated at 37°C and 200 rpm for 1-2 hours. Agar beads were prepared using LB media diluted 1:50 in water containing 1.5% agar. Media was autoclaved for 20 min and equilibrated at 50°C in a water bath. Five milliliters of sterile heavy mineral oil (Sigma-Aldrich) were added to 100 mL glass beakers and equilibrated at 50°C in a water bath. When bacterial cultures were ready, bacterial cells were collected by centrifugation at 14,000 rpm for 1 min, supernatants were discarded, and bacterial cells were resuspended in 100 μL sterile phosphate-buffered saline (PBS). Beakers containing pre-warmed heavy mineral oil were placed on a magnetic stir plate and stirred at 1,050 rpm at room temperature. Bacterial suspensions in PBS were briefly mixed with 900 μL of pre-warmed diluted LB agar, and the mixture was immediately added to the middle of the vortex created while stirring the heavy oil at high speed. The mix was stirred at 1,050 rpm for 3 minutes, and then at 650 rpm for 3 additional minutes. The suspension was transferred to a 4°C cold room and stirred at 50-60 rpm for 35 min, followed by incubation on ice for 20 min. The agar bead suspension was then transferred to 15 mL conical sterile polypropylene centrifuge tubes (Thermo Fisher Scientific), 5 mL of sterile PBS were added, and the suspension was centrifuged at 1,600 × g for 5 min at 4°C. After centrifugation, supernatant containing a visible layer of heavy oil was carefully removed using a 5 mL pipette. The beads were then washed with sterile PBS followed by centrifugation at 1,600 × g for 5 min at 4°C. After 4 washes, the suspension containing the beads was transferred to a clean 15 mL sterile polypropylene centrifuge tube, and 2 additional washes with PBS were done as previously described. Beads were resuspended in 3 mL sterile liquid LB media diluted 1:50 in water containing 300 μg/mL carbenicillin and transferred to sterile tissue culture 6-well plates (Fisher Scientific). The beads were incubated at 70 rpm for 20 hours at 37°C in a Digital Orbital Incubator (Thermo Fisher Scientific) to promote bacterial growth. After overnight incubation, the beads were washed 3-4 times with sterile PBS to remove planktonic bacteria, followed by centrifugation at 520 x g for 1 min at 4°C. The beads were then resuspended in 200 μL 1:50 LB media with 300 μg/mL carbenicillin. Heat-killed beads, used as controls, were prepared as described above using PA14 wild-type bacterial suspensions that had been incubated at 85°C for 1 min before bead preparation. Bacterial cultures were plated on LB agar media after heat treatment to confirm loss of bacterial viability. Agar beads without bacteria were prepared in parallel to serve as negative controls. Bead diameter was measured in different fields using a fluorescent microscope (Nikon Ti2 inverted fluorescent LED phase contrast microscope). Average bead sizes were between 100-200 μm, and beads of 200 μm were selected for swarming assays.

3D imaging of embedded agar beads

The structure and morphology of *Pseudomonas*-embedded beads were analyzed by acquiring z-stack images using fluorescent confocal microscopy at 10x magnification (Nikon C2 Laser-Scanning Confocal microscope mounted on ECLIPSE Ti-E inverted base). Images were rendered into 3D models using the 3D Viewer plugin in FIJI.[60] Image brightness and contrast were adjusted to enhance the visibility of the fluorescent biofilm while minimizing noise. Then, the 3D surface rendering option was selected with a threshold setting of 20, optimizing bead visualization.

Neutrophil isolation

Fresh, deidentified samples of peripheral blood collected from healthy volunteers (Research Blood Components LLC) in 10 mL EDTA tubes were utilized within 6 hours post-draw. Neutrophils were isolated using the EasySep Direct Human Neutrophil isolation kit per the manufacturer's protocol (STEMCELL Technologies). Isolated neutrophils were stained with Hoechst (Thermo Fisher Scientific) and resuspended in Iscove Modified Dulbecco's Medium (IMDM) containing 20% Fetal Bovine Serum (FBS) (Thermo Fisher Scientific) before use for swarming assays. Sytox Deep Red Nucleic Acid Stain (Invitrogen), a high-affinity nucleic acid stain that penetrates cells with compromised plasma membranes, was added at a concentration of 0.5 μM to the neutrophil suspension prior to seeding.

Swarming assay

Swarming assays were performed using glass bottom 12-well plates N° 1.5 coverslip uncoated (MatTek Corporation) and imaged using an automated Nikon TiE fluorescent microscope with Plan Fluor 10x 0.3 NA Ph1 DLL lens. Inside each well of the plate, four 2 mm diameter microwells in 2 × 2 arrays were employed to keep agar beads and neutrophils in close contact. Polydimethylsiloxane (PDMS) sheets of 3 mm thickness were used to fabricate the microwells. Biopsy punches were used to cut 10 mm diameter PDMS cylinders, and four microwells were extracted from each cylinder using a 2 mm biopsy punch. The PDMS microwells were bonded to plasma-treated glass substrates of the 12-well plates. Agar beads were picked under a microscope using a P10 pipette, and one bead was transferred to each microwell containing IMDM with 20% FBS. Neutrophils were added at a concentration

of 2 × 10^7 cells per mL in a 10 μL aliquot of IMDM with 20% FBS. Then, the 12-well plates were transferred to the microscope's heated chamber warmed to 37°C for time-lapse imaging. Swarming targets were selected and saved using the multipoint function in NIS elements prior to the loading of neutrophils (up to 4 replicate beads were imaged for each condition). All selected points were optimized using the Nikon Perfect Focus system before starting the experiment. Images were acquired every 10 minutes over 14 hours.

Area of swarm analysis

Individual neutrophil swarms were segmented manually using the image processing software FIJI (distribution of ImageJ2 core).[61] Each swarm appeared as a distinct bolus of packed neutrophils, which was highlighted using fluorescent microscopy. Dense regions of Hoescht-stained nuclei encompassing a bead were used to identify swarm area boundaries. Areas were segmented over the 14-hour time-lapse and normalized to the initial size of the bead.

Neutrophil cell count analysis using Cellpose cell segmentation

Cellpose (v2.2.2)[62,63], an open-source cell segmentation algorithm, was used to identify, segment, and count Hoechst-stained neutrophil nuclei within each image. Quantification of cells obtained from Hoechst-stained time-lapse images was performed in 375 × 375 μm frames. Average particle diameter for the nuclei model was set to 9 μm. The same field of view was used to analyze all the time points obtained for a given condition. Four frames, one per microwell, were taken per condition/data point and used for Cellpose analysis. Neutrophil nuclei were counted in frames devoid of beads, but proximal to the beads because accurate resolution and quantification of individual nuclei was obscured in areas of packed neutrophils directly adjacent to beads during swarm formation. A decrease in number of resolvable nuclei proximal to a bead over time was interpreted as either loss of nuclei integrity (i.e. cell death) or movement of cells off the frame (i.e. movement into a swarm around a bead).

Extracellular nuclear material quantification by Sytox stain intensity analysis

Fluorescence of Sytox Deep Red Nucleic Acid Stain was measured to assess extracellular nuclear material as an indicator of cell death in the assays. Intensity profiles were measured within each time-lapse frame and plotted over time. Each intensity datapoint was normalized to the initial measurements and biological replicates of each condition were averaged for graphical representation. Additional analyses conducted on this data include comparisons of Sytox Red intensity, rate of intensity change and time points at which 0.2 a.u. (arbitrary units) of relative intensity were reached. A minimum mean intensity of 0.2 a.u. was set in the red channel, where objects less intense were not counted by the analyzer.

LDH cytotoxicity assay

Cytotoxicity was assessed by measuring lactate dehydrogenase (LDH), a stable cytosolic enzyme released upon cell lysis. LDH release in culture supernatants was measured using a coupled enzymatic assay (LDH Cytotoxicity Assay Kit, Thermo Fisher Scientific), which results in the conversion of a tetrazolium salt (INT) into a red formazan product. The amount of formazan product formed, measured by spectrophotometry, is proportional to the number of lysed cells. Swarming assays were performed in 16-well proplates (Grace Bio-Labs) to obtain sufficient supernatant for LDH quantitation. Between 20 and 30 embedded agar beads were individually picked under a microscope using a P10 pipette and transferred to a proplate well containing 100 μL of phenol red free IMDM with 20% heat-inactivated FBS. Neutrophils were added at a concentration of 5 × 10^6 cells per mL in a 100 μL volume of IMDM with 20% heat-inactivated FBS. Triton X-100 (Sigma-Aldrich) at a final concentration of 0.1% was used to determine the Target Cell Maximum LDH Release Control required to calculate 100% release of LDH. Neutrophil only controls were included in the assay. Proplates were incubated at 37°C for 1, 2, 3 and 9 hours. Fifty microliter aliquots from proplate wells were transferred to 96-well flat bottom plates (Fisher Scientific) at the end of the incubation period and used to estimate LDH release following manufacturer protocols. Absorbance was measured with a microplate reader (SpectraMax iD5, Molecular Devices) at 480 nm. Cytotoxicity was expressed as percentage of total amount of LDH released by neutrophils in the culture media.

Cytokine interleukin-1β (IL-1β) ELISA

Swarming assays used to quantify IL-1β production were performed using 16-well proplates as described above for the LDH Cytotoxicity assay, supernatants from the swarming assays were used to quantify both LDH and IL-1β. Between 20-30 *P. aeruginosa* embedded agar beads were individually picked under microscope using a P10 pipette and transferred to proplate wells containing 100 μL of IMDM with 20% heat-inactivated FBS media. Neutrophils were subsequently added at a concentration of 5 × 10^6 cells per well in a 100 μL volume. Neutrophil-only controls were included in the assay. Proplates were incubated at 37°C for 1, 2 3 and 9 hours. The production of IL-1β was quantified using an enzyme-linked immunosorbent assay (R&D Systems). Aliquots of 100 μL from proplates were transferred to 96-well plates (Fisher Scientific), and ELISA assays were performed following manufacturer protocols.

P. aeruginosa survival assay

Survival of bacterial strains was quantified after performing swarming assays in microcentrifuge tubes to ensure recovery of agar beads after the incubation period. One agar bead was individually picked under microscope using a P10 pipette and transferred to 2mL screw-cap microcentrifuge tubes (VWR International) containing 100 μL of IMDM with 20% heat-inactivated FBS. Neutrophils were added at a concentration of 5 × 10^6 cells per mL in 100 μL of IMDM with 20% heat-inactivated FBS. Tubes were incubated at 37°C for 3 hours. Controls without neutrophils were set up after transferring 1 agar bead per tube in 200 μL of IMDM with 20%

heat-inactivated FBS. After the incubation period, a sterile 5 mm stainless-steel bead (Qiagen) and Triton X-100 (Sigma) at a final concentration of 1%, was added to each tube. Disruption of agar beads was accomplished by transferring the tubes to a TissueLyser LT (Qiagen) and applying 3 cycles of 3 minutes at 50 Hz (3000 oscillations/minute) in a 4°C cold room. Aliquots from each tube were then diluted 1:10 into sterile 96-well plates (Thermo Fisher Scientific) containing 180 μL PBS buffer, and serial dilutions were performed. Ten microliter aliquots from each dilution were plated on LB agar media and incubated overnight at 37°C. After incubation, the number of Colony Forming Units (CFUs) was determined for each condition.

QUANTIFICATION AND STATISTICAL ANALYSIS

Statistical analyses were performed using GraphPad Prism 10 and Microsoft Excel software. Data are presented as the mean values ± SD of at least three independent experiments with the following exception: Figures S3A and S3B are representative of two independent experiments. The number of independent replicates for each experiment is outlined in the figure legends. Comparisons between two groups were performed using the two-tailed Student's t test or One Way ANOVA. Statistical significance was considered for $p < 0.05$ and is provided in the relevant figure legends. Error bars represent standard deviation unless otherwise indicated. P values indicating significance are depicted as follows: *$p < 0.05$, **$p < 0.01$, ***$p < 0.001$, ****$p < 0.0001$, ns is non-significant.